Available online at www.sciencedirect.com
SCIENCE DIRECT
Journal of Solid State Chemistry 179 (2006) 1003–1008
JOURNAL OF SOLID STATE CHEMISTRY
www.elsevier.com/locate/jssc

CaB_3—A new calcium boride stabilized by thin film epitaxy

Hiroki Yamazaki*, Hidenori Takagi

Magnetic Materials Laboratory, Discovery Research Institute, RIKEN (The Institute of Physical and Chemical Research), Wako, Saitama 351-0198, Japan

Received 22 August 2005; received in revised form 12 December 2005; accepted 17 December 2005
Available online 20 January 2006

Abstract

Codeposition of Ca and B on various single crystal substrates was carried out by MBE technique. A new calcium boride CaB_3 was epitaxially grown on $Al_2O_3(0001)$ with substrate temperature $T_s = 500\,^{\circ}C$. Structural characterization by RHEED and X-ray diffraction indicated that CaB_3 has a hexagonal cell with lattice parameters $a = 4.088 \pm 0.023$ Å and $c = 4.098 \pm 0.002$ Å. No evidence for superconductivity was found down to 2 K.

Keywords: Molecular beam epitaxy; Codeposition technique; Calcium boride; CaB_3

1. Introduction

The discovery of superconductivity above 39 K in intermetallic MgB_2 [1] has generated considerable interest from both fundamental and technical perspectives. Metallic borides are now a group of materials in the spotlight. It is quite natural that one expects novel properties (including superconductivity) of calcium borides since calcium has a position just below magnesium in the periodic table of the elements. However, to date, CaB_6 (cubic, CaB_6-type) is the only stable phase known in Ca–B binary, partly due to the large ionic radius of Ca^{2+}. The objective of the present study is to explore a new phase of CaB_x ($x \neq 6$) in the form of a thin film. When a thin film is epitaxially grown on a single-crystal substrate, there is a possibility that unstable phase under ordinary conditions can be formed due to epitaxial strain in the film. A theoretical suggestion that a superconducting transition temperature T_c higher than 39 K may be obtained if CaB_2 were stabilized [2] has encouraged us to perform this study.

The technique to prepare CaB_x films in this study is the codeposition of Ca and B onto single-crystal substrates in a MBE chamber, which was successfully applied in the growth of the MgB_2 films [3]. Dependence of structural properties on the film-growth conditions (substrate materials, crystal orientation of the substrate, growth temperature, and deposition-rate ratio) is investigated to determine the optimum growth conditions. A goal is to find a new phase CaB_x other than CaB_6 phase. Though CaB_2 was not obtained, we found a new phase CaB_3 with a hexagonal structure.

2. Experimental

2.1. Sample preparation

Thin films of CaB_x were grown on single-crystal substrates (typically $1 \times 1\,cm^2 \times 0.3$ mm) in a MBE chamber (Eiko Co., Japan) with a base pressure of $1–2 \times 10^{-10}$ Torr. During the deposition, the pressure increased to $1–2 \times 10^{-9}$ Torr mainly due to hydrogen and nitrogen molecules escaped from heated evaporation sources. Before loading to the chamber, the substrate was rinsed in acetone then kept in an O_3 atmosphere for 30 min to remove organic molecules from the surface. Five single-crystal substrates were used: $Al_2O_3(0001)$, $Al_2O_3(11\bar{2}0)$, $Al_2O_3(10\bar{1}0)$, MgO(100), and Si(111). These substrates were heated to 750 °C in vacuum for heat-cleaning and cooled to the growth temperature (the substrate temperature during the film growth) $T_s = 330–550\,^{\circ}C$. Ca metal granules (Johnson Matthey, 99.5%) and B pieces (Johnson Matthey, 99.5%) were used as evaporation sources. Ca was evaporated from an effusion cell kept at 600 °C and B was

*Corresponding author. Fax: +81 48 462 4649.
E-mail address: yamazaki@postman.riken.go.jp (H. Yamazaki).

0022-4596/$ - see front matter © 2005 Elsevier Inc. All rights reserved.
doi:10.1016/j.jssc.2005.12.028

evaporated using an electron-beam gun. Codeposition of Ca ([Ca] = 3.1 Å/s on average) and B ([B] = 1.4–3.4 Å/s) was carried out to a total film thickness of typically 1500 Å, where [Ca] and [B] denote the deposition rates of Ca and B, respectively. [Ca] monitored by a crystal oscillator (INFICON) was quite stable within a range of 0.1 Å/s at least for 30 min, so that [Ca] could be regarded as constant during deposition. Just before the film growth, [Ca] was measured and [B] during growth was calculated from the relation [B] = [Ca + B]-[Ca], where [Ca + B] is the total deposition rate monitored by the crystal oscillator adjacent to the substrate. The normalized Ca deposition rate $r = [Ca]/[B_2]$, where $[B_2] = [B]/2$, was controlled by adjusting [Ca + B]. Film growth was conducted in the range of $0.4 \leqslant r \leqslant 1.1$. Note that one should not take the value of r literally because r was estimated by a crystal oscillator kept at room temperature. On the substrate, the elevated T_s (= 330–550 °C) likely promotes the re-evaporation of Ca, resulting in loss of Ca in the films and simultaneously reduction of the total film thickness from 1500 Å. Since Ca granules were observed to evaporate above 480 °C from an effusion cell in high vacuum, the re-evaporation of Ca from the substrate may accordingly occur for $T_s \geqslant 480$ °C. The CaB_x films, so grown, were always handled in dry N_2 or He gas in order to avoid oxidization after they were taken out of the MBE chamber.

2.2. Characterization

A correlation between structural properties and film-growth conditions was investigated. Four growth conditions were particularly taken into account: substrate materials, crystal orientation of the substrate, T_s, and r. The structure of all the samples was characterized by in-situ reflection high-energy electron diffraction (RHEED) with 15 keV beam intensity and by ex-situ reflection X-ray diffraction with 2θ–θ scans using Cu$K\alpha$ radiation. The optimum growth conditions were determined in consideration of the peak intensity and the structural coherence length obtained from X-ray diffraction measurements. For the films grown under optimum conditions, the following studies were further performed: (1) the quantitative analysis of constituent atoms by RBS/NRA method, where RBS stands for Rutherford Backscattering Spectrometry and NRA for Nuclear Reaction Analysis, and (2) in-plane X-ray diffraction measurements with grazing incidence using Cu$K\alpha$ radiation. NRA was carried out using $B^{11}(p,\alpha)Be^8$ reaction in order to determine the surface concentration of B. Making use of the B concentration, the backscattering spectrum obtained by RBS using a beam of He^4 ions was fitted to a theoretical curve to provide the depth profile of atomic ratio. RBS/NRA was carried out at Toray Research Center, Inc. As preliminary studies on magnetic and superconducting properties of the films, dc magnetization was measured for all the samples using a superconducting quantum interference device magnetometer (Quantum Design MPMS2).

3. Results

3.1. Determination of the optimum growth conditions

To optimize the film growth, CaB_x films were first grown on five different substrates on the same conditions of T_s = 500 °C and $r = 1.0$. The X-ray diffraction patterns of 2θ–θ scans in Fig. 1 were obtained at room temperature for $\boldsymbol{R}\perp$ film-plane, where $\boldsymbol{R}$ stands for the scattering vector. The main peaks of the substrates are distinguished by inverted triangles. We have confirmed that the small peak at ~65° for $Al_2O_3(0001)$ is also of substrate origin. The films on the $Al_2O_3(0001)$ and Si(111) substrates exhibit a single phase with a peak at ~22° and its higher-order peak at ~44° indicated by broken lines; while broad peaks other than these two peaks are observed for the other substrates. This result shows that the CaB_x films make a better match for a hexagonal surface of $Al_2O_3(0001)$ and Si(111) than for a rectangular (or square) surface of $Al_2O_3(11\bar{2}0)$, $Al_2O_3(10\bar{1}0)$, and MgO(100). When we compare $Al_2O_3(0001)$ and Si(111), the peak intensity of the film on the former is about one order of magnitude larger than that on the latter. This suggests richer crystallinity of the film on $Al_2O_3(0001)$ than on Si(111). The lattice spacing calculated from the peak at ~44° is 2.049 ± 0.001 Å for $Al_2O_3(0001)$ and 2.055 ± 0.001 Å for Si(111). Compared with the film on $Al_2O_3(0001)$, the film on Si(111) is slightly (~0.3%) expanded in the lattice spacing likely due to the epitaxial

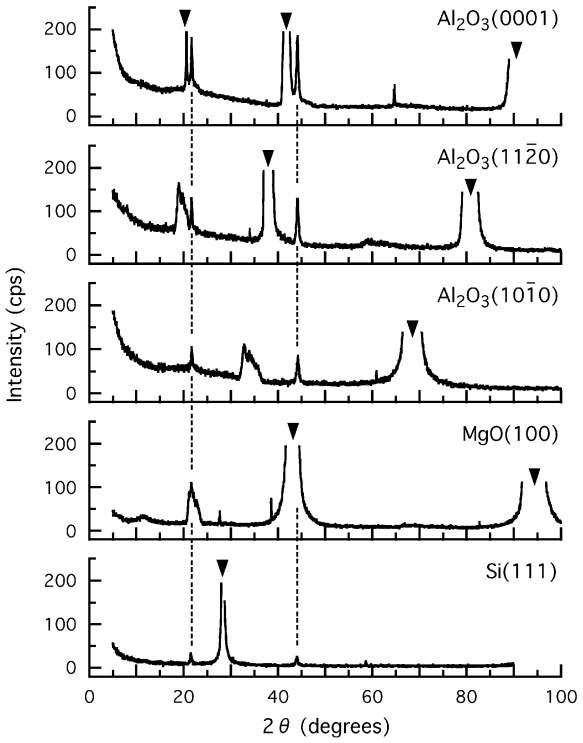

Fig. 1. Substrate dependence of the reflection X-ray diffraction patterns observed for the samples grown at T_s = 500 °C and $r = [Ca]/[B_2] = 1.0$. The peaks distinguished by inverted triangles are of substrate origin.

strain that compresses the film in the direction parallel to its plane. We see that one can obtain the best result when the $Al_2O_3(0001)$ substrate is used for the growth of the CaB_x film.

The lattice spacing of 2.049 Å observed for $Al_2O_3(0001)$ is close to 2.077 Å for bulk $CaB_6(200)$ (Ref. [4]) but cannot be due to CaB_6. As we will see in Section 3.2, the depth profile of atomic ratio shows that the CaB_x film grown under optimum conditions has a uniform value of $x = 3.3 \pm 0.2$ independent of depth in the film. A possibility of the growth of CaB_6 film due to intense re-evaporation of Ca or a complete phase separation of CaB_6 and Ca in the film can be therefore excluded. It is hard to imagine that granules of CaB_6 crystals, which are all arranged with their (100) plane parallel to the film plane, are embedded in a Ca matrix uniformly.

Using the $Al_2O_3(0001)$ substrate that has been observed to make the best match with the CaB_x film, the optimum r and T_s with respect to film crystallinity were determined. For a fixed $T_s = 500\,^{\circ}C$, the structural coherence length perpendicular to the film plane ($\xi_\perp$) and the diffraction-peak intensity were derived as a function of r from the peak at ~44° in the 2θ–θ scan of X-ray diffraction for $\boldsymbol{R}\perp$ film-plane. The value of $\xi_\perp$ was calculated from the relation $\xi_\perp = 2\pi/\Delta Q$, where ΔQ is the full-width at half-maximum (FWHM) of the intensity profile as a function of the wave number Q. The largest values of $\xi_\perp$ and peak intensity, namely the richest crystallinity, are obtained at $r = 1.0$ (see Fig. 2). For $r < 0.9$, distinct diffraction peaks were not observed. A slight change of r from 1.0 to 0.9 or 1.1 causes about 60% reduction in the peak intensity. This appears to imply that a stoichiometric composition is realized at $r = 1.0$. On the basis of the stoichiometric composition at $r = 1.0$, we have a Ca-deficient film at $r = 0.9$ and a Ca-rich one at $r = 1.1$. As we can see in Fig. 3, for a fixed $r = 1.0$, a deviation of T_s from 500 °C causes much degradation of the crystallinity. Distinct diffraction peaks were not observed for $T_s < 400\,^{\circ}C$.

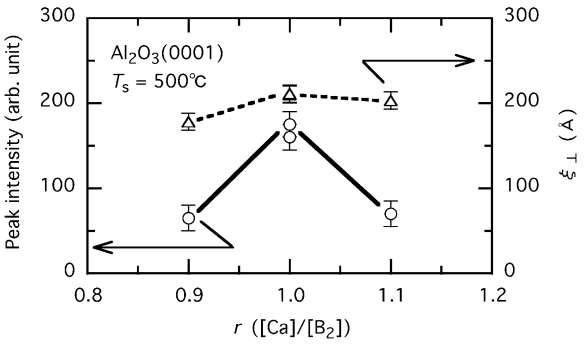

Fig. 2. Determination of the optimum r for the CaB_x films grown on the $Al_2O_3(0001)$ substrate at $T_s = 500\,^{\circ}C$. The structural coherence length perpendicular to the film plane ($\xi_\perp$) and the peak intensity are shown as functions of r.

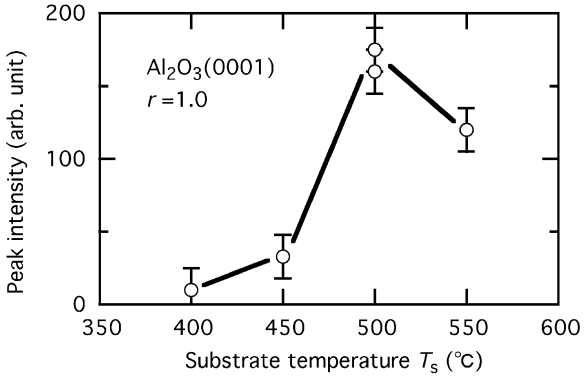

Fig. 3. Dependence of the X-ray diffraction peak intensity on the substrate temperature T_s for the CaB_x films grown on the $Al_2O_3(0001)$ substrate at $r = 1.0$.

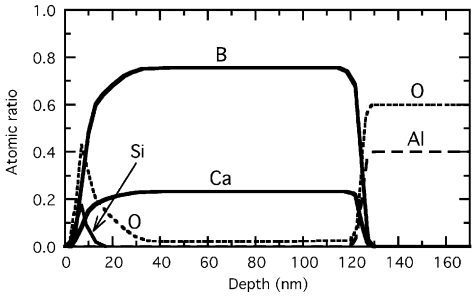

Fig. 4. Depth profile of atomic ratio obtained by RBS/NRA method for the CaB_x film grown under optimum conditions: $Al_2O_3(0001)$ substrate, $T_s = 500\,^{\circ}C$, and $r = 1.0$.

3.2. Quantitative analysis of constituent atoms

As has been already mentioned in Section 2.1, the value of r does not always correspond to the real composition ratio of Ca to B in the film since one cannot disregard the re-evaporation of Ca from the film. It is crucial for the present study to determine a real stoichiometric composition of the CaB_x film by quantitative analysis of constituent atoms. For the sample grown under optimum conditions, the depth profile of atomic ratio in Fig. 4 was obtained by means of RBS/NRA method. The depth can be determined to an accuracy of the order of 10 nm. The profiles of Ca and B atoms indicate that the CaB_x film has a uniform value of $x = 3.3 \pm 0.2$ independent of depth in the film implying the empirical formula of $CaB_{3.3\pm0.2}$. For the depths above 125 nm, the response of Al and O atoms in the ratio Al:O = 2:3 is attributed to the Al_2O_3 substrate. The concentration of Si and O atoms in the vicinity of the surface is due to silicone grease adhered to the film surface accidentally, so that it is not intrinsic to the film. We notice, however, a slight but persistent response of O in the CaB_x film from 40 to 120 nm with an atomic ratio of ~0.02. A possibility is that this small amount of oxygen came from the substrate in the growth process of the film.

3.3. Structural characterization

In order to obtain quantitative information on the lattice structure, in-plane X-ray diffraction study was performed for the stoichiometric film grown under optimum conditions. The angle of X-ray grazing incidence was set at 0.3°. Typical diffraction patterns are shown in Fig. 5 for two directions of the scattering vector $\boldsymbol{R}$. In the insets of Fig. 5, these directions are indicated as thick arrows in the coordinates of the $Al_2O_3(0001)$ substrate. The notation $2\theta\chi$ denotes the scattering angle in the plane. The peaks marked with inverted triangles, including the shoulders on the right side of the $Al_2O_3(300)$ and $Al_2O_3(220)$ peaks, are of substrate origin. This was confirmed in comparison with the diffraction patterns of the substrate alone. For $\boldsymbol{R}||\langle 1\bar{1}00\rangle$ (upper panel), we recognize two peaks (distinguished by the triangles at ~26° and ~52°) which are of CaB_x origin. It may be hard to distinguish the lower-angle peak because it is close by the substrate peak at ~30° and the background inclines steeply, but a broad peak is distinguished from the background after subtraction of the substrate contribution (the diffraction obtained for the substrate alone). The broad peak can be fitted to the Gaussian distribution with a peak at 26°(±2°) and the FWHM of 4.2°(±1.3°), where the values in the parentheses indicate the errors. The existence of in-plane diffraction peaks indicates the structural order in the film plane implying the epitaxial growth of the film on the substrate. From the peak at ~52°, the in-plane lattice spacing $d_{\parallel} = 1.77 \pm 0.01$ Å and the in-plane structural coherence length $\xi_{\parallel}$~20 Å were obtained. This small value of $\xi_{\parallel}$ may be attributed to a large amount of dislocation, which could produce the lattice relaxation in the highly strained film due to heteroepitaxy and could be anisotropic depending on the crystal direction in the film plane. For the direction parallel to $\langle 11\bar{2}0\rangle$, the in-plane structural coherence length may be shorter than 20 Å yielding the broadening out of the diffraction peaks for $R||\langle 11\bar{2}0\rangle$. This can explain why we cannot observe any peaks of CaB_x origin in the lower panel of Fig. 5. Taking the result of $\xi_{\perp}$~210 Å (see Fig. 2) for the same sample into account, a section of structural coherence approximately takes the cylindrical form of ~210 Å in axis and ~20 Å (or shorter than this in the $\langle 11\bar{2}0\rangle$ direction) in diameter. The axes of the cylindrical sections have an angle distribution centering on the normal of the film plane with a FWHM about 5°, which was estimated from the FWHM of the rocking curve for the ~44° peak observed for $\boldsymbol{R}\perp$ film-plane (the top panel of Fig. 1).

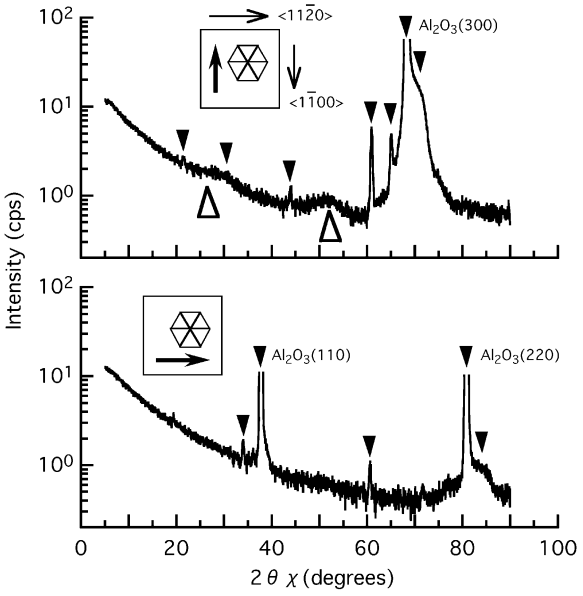

Fig. 5. In-plane X-ray diffraction patterns obtained for the sample grown under optimum conditions: $Al_2O_3(0001)$ substrate, $T_s = 500$ °C, and $r = 1.0$. The peaks marked with filled inverted triangles are those of substrate. Insets: directions of the scattering vector $\boldsymbol{R}$ in the coordinates of the $Al_2O_3(0001)$ substrate.

The in-plane X-ray diffraction study mentioned above could not provide sufficient information to determine the lattice structure of the CaB_x film. Laue method was not successfully applied either due to hardly detectable diffraction from the film in contrast to the intense spots from the substrate. The lattice structure was, therefore, explored with the help of in-situ RHEED. The spot diffraction in Fig. 6(a) was observed for the stoichiometric film grown under optimum conditions. As growth conditions deviate from the optimum ones, the spot diffraction changed into the ring diffraction gradually. The spot diffraction implies that the film surface is not flat and the diffraction is from transmission through the protuberances

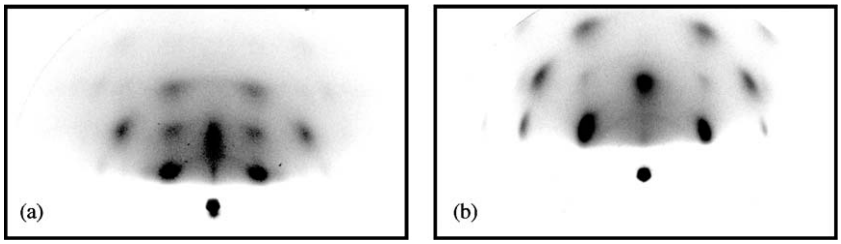

Fig. 6. Reversal images of the RHEED observed for the surface of (a) stoichiometric CaB_x film and (b) MgB_2 film (reference sample [3]). Both have been grown on the $Al_2O_3(0001)$ substrate in common under individual optimum conditions. The direction of the incident electron beam is parallel to $\langle 11\bar{2}0\rangle$ of the $Al_2O_3(0001)$ substrate.

of the surface. Surface roughness of this degree seems to be inevitable for the films of metallic boride when they are grown by the codeposition technique. The RHEED image of the MgB_2 film of $T_c = 27\,K$ (Ref. [3]) is shown in Fig. 6(b) for reference. This film was also prepared on the $Al_2O_3(0001)$ substrate by basically the same method as the CaB_x films. The direction of the incident electron beam was parallel to $\langle 11\bar{2}0\rangle$ of the $Al_2O_3(0001)$ substrate in common with Fig. 6(a). We recognize the spot diffraction for the MgB_2 film, too. Attention should be paid also to a similarity in the pattern of spots between CaB_x and MgB_2 except that the two spots on both sides of the center one are weak (or maybe hardly visible in the printed page) for MgB_2 as compared with those for CaB_x. Since the MgB_2 film is preferentially oriented parallel to the hexagonal c-plane of the AlB_2 structure [3], this similarity implies a possibility that the CaB_x film has a hexagonal surface-lattice, which is consistent with the result that the CaB_x films make a good match for a hexagonal surface of the $Al_2O_3(0001)$ and Si(111) substrates (Section 3.1). We will confirm this hypothesis below.

Provided that difference in the size of RHEED pattern between MgB_2 and CaB_x is attributed to that in size of the primitive cell of the crystal lattice, judging from the horizontal intervals between the spots, the in-plane primitive cell of the CaB_x film is 1.34 ± 0.03 times as large as that of the MgB_2 film. The lattice constant a is consequently calculated for the hexagonal surface-lattice of CaB_x: $a = 3.08831\,Å \times (1.34 \pm 0.03) = 4.14 \pm 0.10\,Å$, where the lattice constant of 3.08831 Å for bulk MgB_2 (Ref. [5]) is used. For $a = 4.14 \pm 0.10\,Å$, the (200) diffraction in the hexagonal lattice corresponds to the lattice spacing of $1.79 \pm 0.04\,Å$, which well agrees with the in-plane lattice spacing of $d_{\parallel} = 1.77 \pm 0.01\,Å$ for the peak at $\sim 52^\circ$ in the upper panel of Fig. 5. The two peaks at $\sim 26^\circ$ and $\sim 52^\circ$ observed in the in-plane diffraction are now identified as the (100) and (200) peaks in the hexagonal lattice.

The possibility that CaB_x is face-centered cubic with its (111) plane parallel to the film plane should be examined. If CaB_x were face-centered cubic, we would have the relation $c = \sqrt{6}a$ in the hexagonal notation. The two diffraction peaks observed for $\boldsymbol{R}\perp$ film-plane (see the top panel of Fig. 1), however, indicate a lattice spacing of $4.098 \pm 0.002\,Å$ in contrast to $c = \sqrt{6}a = 10.014\,Å$ for $a = 4.088\,Å$ (calculated newly from $d_{\parallel}$). These peaks for $\boldsymbol{R}\perp$ film-plane can be regarded as the (001) and (002) peaks in the hexagonal lattice. It is now evident that the hexagonal lattice with $a = 4.088 \pm 0.023\,Å$ and $c = 4.098 \pm 0.002\,Å$ explains the results of RHEED and X-ray diffraction measurements consistently.

3.4. Determination of the number of the chemical units constituting the unit cell

Since the surface concentration of B atoms, $\rho = (4.68 \pm 0.33) \times 10^{17}\,cm^{-2}$, was measured by NRA, the number of B atoms in the unit cell, n, can be estimated by the relation $n = (\rho v)/V$, where $v(= \sqrt{3}a^2c/2)$ is the unit-cell volume of the hexagonal lattice and V is the volume of the CaB_x film of $1\,cm^2$ in area. For the film thickness of $110 \pm 10\,nm$ (estimated from the depth profile of atomic ratio in Fig. 4), we obtain $n = 2.53 \pm 0.30$. If we define z as the number of the chemical units constituting the unit cell, there are $Ca \times z$ and $B \times zx$ atoms in the unit cell and the expression $n = zx$ holds for B atoms. Since the quantities of n and z should be integers and we have $x = 3.3 \pm 0.2$ (Section 3.2), a combination of $n = 3$, $z = 1$, and $x = 3$ is uniquely determined considering the errors of the experimental values into account. We can now conclude that a calcium boride of CaB_3 is realized in the film and one Ca atom and three B atoms compose the unit cell of hexagonal lattice.

3.5. Magnetic and superconducting property of the CaB_3 film

In order to examine the magnetic and/or superconducting properties of the new phase of CaB_3 and the Ca-deficient and Ca-rich phases of $CaB_{3\pm\delta}$, dc magnetization measurements were performed for all the samples prepared in this study. The temperature dependence (typical temperature range: 2–50 K) of the magnetization was measured for warming (after zero-field cooling) and cooling procedures in a magnetic field (2–5000 Oe) applied perpendicular to the film plane. Within experimental accuracy, these measurements proved that both CaB_3 and $CaB_{3\pm\delta}$ do not exhibit magnetism. Diamagnetic behavior due to the Meissner effect was not observed. Electric resistivity at room temperature indicates that CaB_3 is conductive with a resistivity less than $10^{-2}\,\Omega\,cm$.

4. Conclusions

A new phase of calcium boride, CaB_3, was realized in a thin film prepared by the codeposition of Ca and B onto the single crystal substrate of $Al_2O_3(0001)$. The optimum film-growth conditions were $T_s = 500\,^\circ C$ and $r = 1.0$ judging from the crystallinity of the film, where T_s is the substrate temperature during the film growth and r is the normalized Ca deposition rate $[Ca]/[B_2]$. Structural studies by RHEED and reflection/in-plane X-ray diffraction implied that the lattice structure of CaB_3 is hexagonal with $a = 4.088 \pm 0.023\,Å$ and $c = 4.098 \pm 0.002\,Å$. It was also confirmed that the unit cell of the hexagonal lattice is composed of one Ca atom and three B atoms. More accurate analysis of the crystal structure such as the determination of atom positions in the unit cell may be difficult due to limited diffraction peaks from the film. Both stoichiometric CaB_3 and nonstoichiometric $CaB_{3\pm\delta}$ did not exhibit any trace of superconductivity or ferromagnetism down to 2 K. For future work, we have to improve the quality of the sample by, for example, selecting

more suitable substrates. This will make it possible to perform structural characterization in detail.

Acknowledgments

The measurements of RBS/NRA were carried out at Toray Research Center, Inc.

References

[1] J. Nagamatsu, N. Makagawa, T. Muranaka, Y. Zenitani, J. Akimitsu, Nature (London) 410 (2001) 63.
[2] N.I. Medvedeva, A.L. Ivanovskii, J.E. Medvedeva, A.J. Freeman, Phys. Rev. B 64 (2001) 020502(R).
[3] H. Yamazaki, Y. Hikita, H. Hori, H. Takagi, Appl. Phys. Lett. 83 (2003) 3740.
[4] Natl. Bur. Stand. (US), Monogr. 25 (16) (1979) 29.
[5] E. Nishibori, M. Takata, M. Sakata, H. Tanaka, T. Muranaka, J. Akimitsu, J. Phys. Soc. Jpn. 70 (2001) 2252.